Nuclear Instruments and Methods in Physics Research B 557 (2024) 165527

Contents lists available at ScienceDirect

Nuclear Inst. and Methods in Physics Research, B

journal homepage: www.elsevier.com/locate/nimb

Full Length Article

Measurement of the $^{10}B(d,\alpha_0)^8Be$, $^{10}B(d,\alpha_1)^8Be^*$, $^{10}B(d,p_2)^9Be^*$, $^{11}B(d,\alpha_0)^9Be$, and $^{11}B(d,\alpha_2)^9Be^*$ reactions cross-sections at the deuteron energies up to 2.2 MeV

Sergey Taskaev [a,b,c,*], Victor Bessmeltsev [d], Marina Bikchurina [a,b], Timofey Bykov [a,b], Dmitrii Kasatov [a,b], Iaroslav Kolesnikov [a,b], Alexey Nikolaev [e], Efim Oks [e,f], Georgii Ostreinov [a,b], Sergey Savinov [a,b], Anna Shuklina [a,b], Evgeniia Sokolova [a,b], Georgy Yushkov [e]

[a] *Budker Institute of Nuclear Physics, 11 Lavrentiev Ave., 630090 Novosibirsk, Russia*
[b] *Novosibirsk State University, 2 Pirogov Str., 630090 Novosibirsk, Russia*
[c] *Joint Institute for Nuclear Research, 6 Joliot-Curie Str., 141980 Dubna, Russia*
[d] *Institute of Automation and Electrometry, 1 Koptyug Ave., 630090 Novosibirsk, Russia*
[e] *Institute of High Current Electronics, 2/3 Akademicheskii Ave., 634055 Tomsk, Russia*
[f] *Tomsk State University of Control Systems and Radio-Electronics, 74 Vershinin Str., 634034 Tomsk, Russia*

ARTICLE INFO

Keywords:
Cross-section
Deuteron beam
Boron target

ABSTRACT

The deuteron-boron fusion reaction produces many different charged particles. Data on the reactions cross-sections differ among different authors, so obtaining experimental data is still relevant. Measurements of the reactions cross-section were carried out at the accelerator-based neutron source VITA at Budker Institute of Nuclear Physics (Novosibirsk, Russia) using an α-spectrometer. The $^{10}B(d,\alpha_0)^8Be$, $^{10}B(d,\alpha_1)^8Be^*$, $^{10}B(d,p_2)^9Be^*$, $^{11}B(d,\alpha_0)^9Be$, and $^{11}B(d,\alpha_2)^9Be^*$ reactions cross-sections at the deuteron energies up to 2.2 MeV have been measured. The obtained data are presented in tabular form.

1. Introduction

The interaction of the deuteron with boron leads to numerous reactions, some of which have been studied in detail [1–25], while others require some clarification. This article is devoted to the measurement of cross-sections of the following nuclear reactions: $^{10}B(d,\alpha_0)^8Be$, $^{10}B(d,\alpha_1)^8Be^*$, $^{10}B(d,p_2)^9Be^*$, $^{11}B(d,\alpha_0)^9Be$, $^{11}B(d,\alpha_2)^9Be^*$.

2. Experimental facility

We previously measured the $^{11}B(p,\alpha_0)^8Be$ and the $^{11}B(p,\alpha_1)^8Be^*$ reactions cross-sections and published the results of the study [26]. To carry out these studies, the same facility [27,28], the same boron target and the same equipment were used. The only thing that was changed was that a deuteron beam was used instead of a proton beam. The deuteron beam current irradiating the boron target was typically 1.2 μA to 1.8 μA (minimum 0.9 μA, maximum 2.2 μA); its stability was at 0.4 %. The facility, the boron target and the equipment, as well as methods for measuring boron thickness are described in detail in the published article [26]. The deuteron beam parameters and methods for determining them are described in detail in the published article [29].

Below are the main characteristics that are important for understanding. The intensity and energy of charged particles (reaction products) were measured by the α-spectrometer with silicon semiconductor detector PDPA-1K (Institute of Physical and Technical Problems, Dubna, Russia). Sensitive surface area of the detector is $S = 20 \pm 1$ mm^2, energy resolution – 13 keV, energy equivalent of noise – 7 keV, capacity – 30 pF, entrance window thickness – 0.08 μm, standard natural background in the range of 3–8 MeV – 0.15 imp/cm^{2}h. The stopping foil was not utilized as the detector input. The measurements were carried out with two options for placing the α-spectrometer: at the angle of 135° at the distance of $R = 717 \pm 1$ mm from the place of generation of charged particles from boron, and at the angle of 168° at the distance of $R = 707 \pm 1$ mm. The solid angles are $\Omega_{lab} = S/R^2 = 3.89 \times 10^{-5}$ sr at the angle of 135° and $\Omega_{lab} = 4.00 \times 10^{-5}$ sr at the angle of 168°, where $S = 20 \pm 1$ mm^2. The accuracy of solid angle measurement is determined by the measurement error of the spectrometer detector area and is 5 %. We consider the detection efficiency of α-particles to be equal to 100 %.

* Corresponding author at: 11 Lavrentiev Ave., 630090 Novosibirsk, Russia.
E-mail address: taskaev@inp.nsk.su (S. Taskaev).

https://doi.org/10.1016/j.nimb.2024.165527
Received 8 July 2024; Received in revised form 13 August 2024; Accepted 7 September 2024

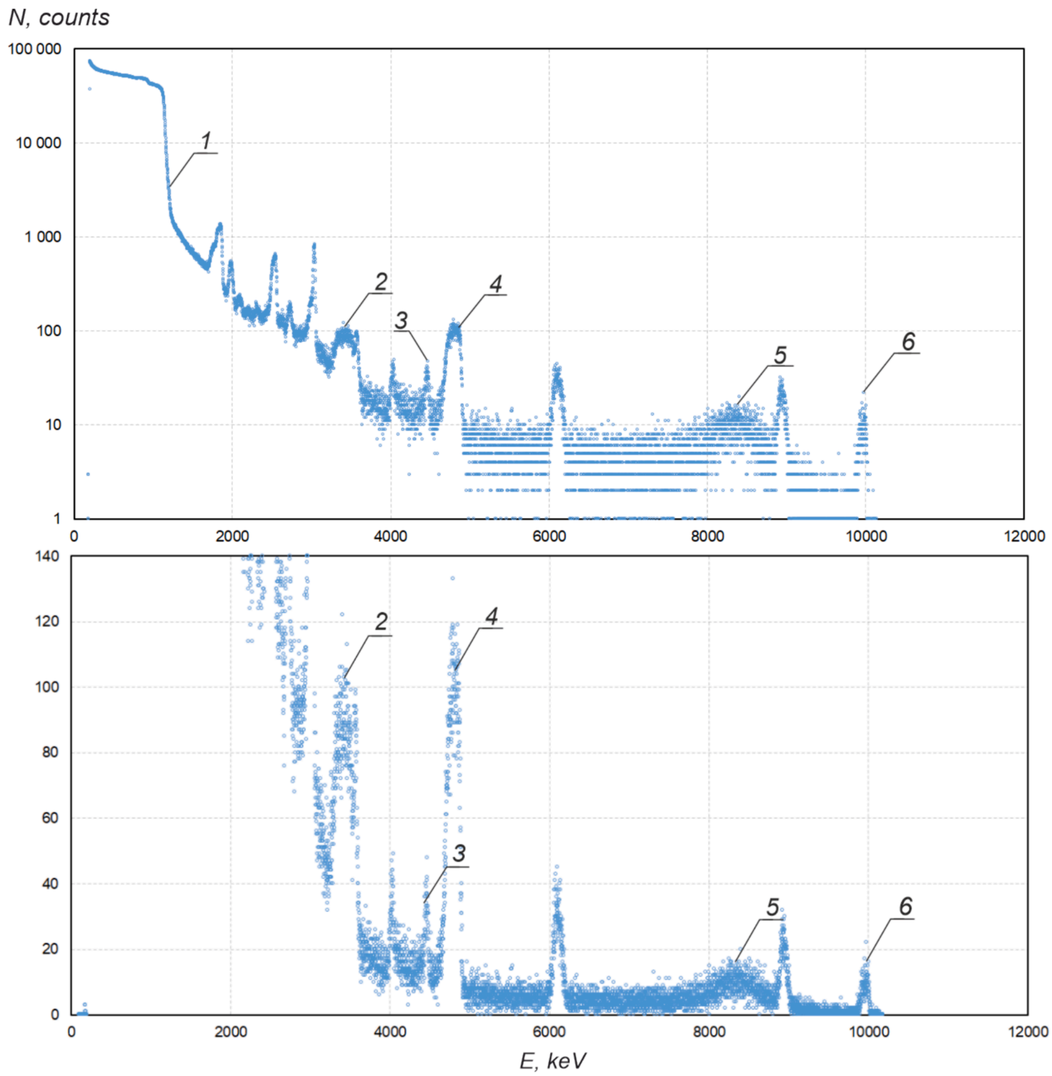

Fig. 1. The signal of the α-spectrometer at 1.5 MeV deuteron beam and 135°: *1* – deuterons backscattered on copper substrate of target, *2* – ^{11}B(d,α_2)^{9}Be* reaction α-particles, *3* – ^{10}B(d,p_2)^{9}Be* reaction protons, *4* – ^{11}B(d,α_0)^{9}Be reaction α-particles, *5* – ^{10}B(d,α_1)^{8}Be* reaction α-particles, *6* – ^{10}B(d,α_0)^{8}Be reaction α-particles.

We will assume the boron layer thickness equal to $(9.0 \pm 0.9) \times 10^{18}$ atoms/cm^2 (0.7 ± 0.07 μm boron crystalline density). The content of ^{11}B isotope is considered equal to 80.2 %.

3. Reactions

When a deuteron interacts with a boron nucleus, the following nuclear reactions occur [30]:

^{10}B + d = α + ^{8}Be + 17.8198 MeV;
^{10}B + d = α + ^{8}Be* + 14.7798 MeV;
^{10}B + d = α + α + α + 17.9117 MeV;
^{10}B + d = p + ^{11}B + 9.2296 MeV;
^{10}B + d = γ + ^{12}C + 25.1864 MeV;
^{10}B + d = n + ^{11}C + 6.4648 MeV;
^{11}B + d = p + ^{12}B + 1.1453 MeV;
^{11}B + d = n + ^{12}C + 13.7323 MeV;
^{11}B + d = α + ^{9}Be + 8.0314 MeV;
^{11}B + d = α + ^{8}Be* + 5.6024 MeV;
^{11}B + d = n + α + α + α + 6.4579 MeV.

The reaction of interaction of a deuteron with boron-10 nucleus forming protons can occur either as a sequential decay via the ground state of ^{11}B, ^{10}B(d,p_0)^{11}B, or via six excited state, ^{10}B(d,p_{1-6})^{11}B*. A typical spectrum from the α-spectrometer is shown in Fig. 1.

The signal in channels below 1.2 MeV is due to deuterons backscattered from the copper substrate of boron target, including double events. Since the cross-sections of a number of reactions of boron-deuteron interactions are relatively low and therefore partially or completely overlap in the spectrum with the signal from elastically reflected deuterons, as well as with the signal from numerous reactions of the deuteron with nitrogen, in this article we focus on measuring the cross–sections of five reactions: ^{10}B(d,α_0)^{8}Be, ^{10}B(d,α_1)^{8}Be*, ^{10}B(d,p_2)^{9}Be*, ^{11}B(d,α_0)^{9}Be, and ^{11}B(d,α_2)^{9}Be*. Unmarked peaks in Fig. 1 are caused by reactions of deuteron with oxygen (~1.85, 2.5 MeV), carbon (~3.0 MeV), nitrogen (~1.8, 2, 2.1, 3.6, 4.1, 6.05, 8.9 MeV), and boron (~2.3, 2.7, 4.0, 6.05 MeV).

4. Measuring reaction cross-sections

The cross-sections of the reactions ^{10}B(d,α_0)^{8}Be, ^{10}B(d,α_1)^{8}Be*, ^{10}B(d,p_2)^{9}Be*, ^{11}B(d,α_0)^{9}Be, and ^{11}B(d,α_2)^{9}Be* was measured as follows. A thin layer of boron was irradiated with a deutron beam, and the α-spectrometer measured charged particles emitted at a certain solid angle. The differential cross–section of the reaction in the laboratory coordinates dσ/dΩ was found from the formula:

$$\frac{d\sigma}{d\Omega} = \frac{eY}{Nknl\Phi\,\Omega_{lab}},$$

Table 1
Measured yield of charged particles Y of ^{10}B(d,α_0)^{8}Be, ^{10}B(d,α_2)^{8}Be*, ^{10}B(d,p_2)^{9}Be*, ^{11}B(d,α_0)^{9}Be and ^{11}B(d,α_2)^{9}Be* reactions at 135° and 168°: E – the average energy of the deuteron interacting with boron atomic nuclei, ΔE – the standard deviation of E, T_{total} – the total measurement time, T_{live} – the live time measurement by α-spectrometer, Φ – the deuteron fluence.

E, keV	ΔE, keV	T_{total}, s	T_{live}, s	Φ, mC	Y, counts				
					^{10}B(d,α_0)^{8}Be	^{10}B(d,α_1)^{8}Be*	^{10}B(d,p_2)^{9}Be*	^{11}B(d,α_0)^{9}Be	^{11}B(d,α_2)^{9}Be*
135°									
369	41	3605	3582	1.47	34	179	57	287	292
467	35	3605	3500	2.22	36	759	240	1217	1282
567	33	4135	3952	2.15	234	1157	560	3035	2616
671	30	3608	3453	1.35	224	1090	437	3509	2693
773	28	3605	3447	1.19	362	1581	504	4934	3481
875	26	3637	3462	1.25	502	2114	796	7517	5138
977	24	4183	4023	1.08	543	2165	863	9141	7000
1078	23	3502	3334	1.12	702	2573	955	12,346	8117
1180	22	3541	3367	1.16	773	3183	955	13,738	9023
1282	20	3485	3318	1.12	779	3484	938	14,112	9854
1382	20	2788	2656	0.89	643	2792	541	11,662	9610
1481	19	3598	3441	1.05	847	4041	809	13,703	11,342
1583	18	3607	3448	1.08	862	4471	754	15,007	10,321
1684	17	3590	3431	1.09	1058	4425	839	16,586	9543
1784	17	3574	3413	1.11	1120	4645	1004	20,323	11,162
1885	16	3576	3407	1.18	1408	5340	1022	23,553	12,598
1987	15	3734	3567	1.18	1543	5592	1173	21,937	11,749
2087	15	3721	3562	1.13	1546	5643	1148	18,481	11,560
2185	15	3635	3491	1.03	1486	5718	1100	15,802	9898
168°									
360	41	3611	3603	0.95	13	89	23	87	135
467	35	19,612	19,293	7.06	220	1245	598	2237	3010
567	33	21,880	21,211	9.38	592	2905	1605	7663	9130
670	30	7225	7005	2.63	208	1322	578	4409	4156
772	28	3607	3476	1.32	166	876	411	3701	3106
874	26	3608	3444	1.64	236	1181	658	6905	4956
977	24	3608	3456	1.62	334	1378	895	9862	6108
1078	23	3607	3487	1.28	329	1233	819	10,372	7390
1180	22	3607	3492	1.22	300	1290	1045	12,251	7979
1282	20	3608	3487	1.31	317	1736	1115	14,765	9406
1383	20	3609	3494	1.26	297	2327	923	14,908	10,055
1481	19	3608	3486	1.38	286	2639	1140	16,950	10,983
1583	18	3611	3497	1.28	245	2695	1021	17,448	9338
1683	17	3634	3476	1.86	317	4168	1859	26,704	13,170
1784	17	3725	3569	1.85	368	4455	1837	30,924	14,829
1885	16	3610	3471	1.66	372	4276	1696	30,753	13,105
1987	15	3607	3456	1.85	451	5710	2151	25,524	15,046
2085	15	3598	3454	1.81	496	5726	2155	22,474	17,932
2185	15	3603	3481	1.52	436	5467	1899	15,248	12,676

where e – the elementary charge, Y – the experimental yield of charged particles (integrated peak counts), N – the number of measured charged particles in the reaction, k – the efficiency of registration of charged particles by the spectrometer ($k = 1$), nl – the linear density of B nuclei ($nl = 7.2 \times 10^{18}$ cm^{-2} for ^{11}B nuclei with the accuracy of 10 %), Φ – the deuteron fluence (accuracy of 1 %), Ω_{lab} – the solid angle ($\Omega_{lab} = 3.89 \times 10^{-5}$ sr at the angle of 135°; $\Omega_{lab} = 4.00 \times 10^{-5}$ sr at the angle of 168° with the accuracy of 5 %).

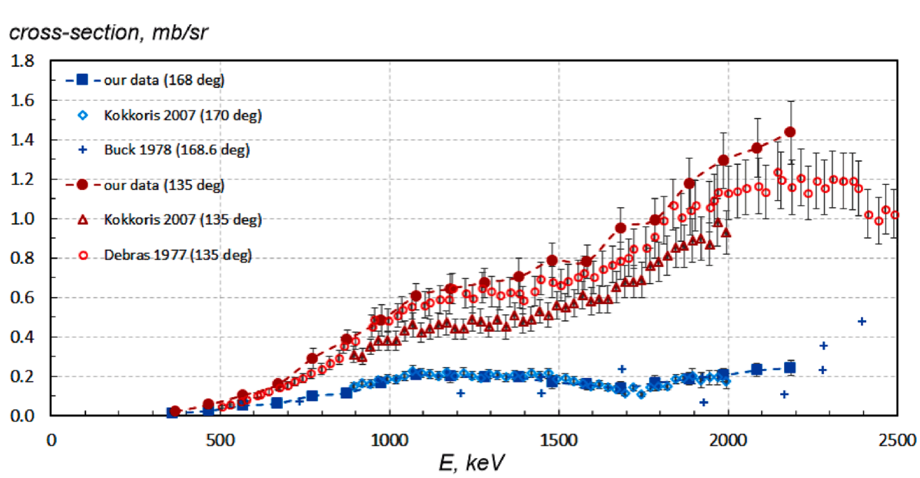

Fig. 2. The measured differential cross-section of the ^{10}B(d,α_0)^{8}Be reaction. Differential cross-sections are in the center-of-mass system.

Table 2
The differential cross-section of the $^{10}B(d,\alpha_0)^8Be$ reaction (in the center-of-mass system) at 135°: E – the deuteron energy, ΔE – the standard deviation of E, σ – the cross-section, Δσ – the statistical variance of σ.

E, keV	ΔE, keV	σ, mb/sr	Δσ, mb/sr
369	41	0.021	0.003
467	35	0.055	0.009
567	33	0.10	0.01
671	30	0.16	0.03
773	28	0.29	0.05
875	26	0.38	0.05
977	24	0.48	0.08
1078	23	0.60	0.07
1180	22	0.64	0.07
1282	20	0.67	0.07
1382	20	0.70	0.09
1481	19	0.79	0.09
1583	18	0.78	0.09
1684	17	0.95	0.10
1784	17	0.99	0.11
1885	16	1.18	0.13
1987	15	1.30	0.14
2087	15	1.36	0.15
2185	15	1.44	0.16

Table 3
The differential cross-section of the $^{10}B(d,\alpha_0)^8Be$ reaction (in the center-of-mass system) at 168°: E – the deuteron energy, ΔE – the standard deviation of E, σ – the cross-section, Δσ – the statistical variance of σ.

E, keV	ΔE, keV	σ, mb/sr	Δσ, mb/sr
360	41	0.010	0.004
467	35	0.024	0.003
567	33	0.050	0.005
670	30	0.063	0.008
772	28	0.10	0.01
874	26	0.12	0.02
977	24	0.17	0.02
1078	23	0.21	0.03
1180	22	0.20	0.03
1282	20	0.20	0.03
1383	20	0.19	0.02
1481	19	0.17	0.03
1583	18	0.16	0.03
1683	17	0.14	0.03
1784	17	0.17	0.04
1885	16	0.19	0.03
1987	15	0.21	0.03
2085	15	0.23	0.03
2185	15	0.24	0.04

The relationship of the differential cross-section in the center of mass system $d\sigma_{c.m.}/d\Omega_{c.m.}$ and in the laboratory coordinates $d\sigma/d\Omega$ is given by the formula [31]:

$$\frac{d\sigma_{c.m.}}{d\Omega_{c.m.}} = \frac{|1+\beta\cos\theta|}{\left(1+\beta^2+2\beta\cos\theta\right)^{\frac{3}{2}}}\frac{d\sigma}{d\Omega},$$

where $\beta = \sqrt{\frac{m_d\widetilde{M}}{M_B M}\bullet\frac{T_M}{T_M+Q}}$ and $T_M = E_d\frac{M}{(m_d+M)}$, M, $\widetilde{M}$ – the masses of decay particles, m_d – the deuteron mass, M_B – the mass of the target particle, in this case mass of B nuclei, θ – the particle detection angle in the laboratory coordinates, in this case 135° or 168°, Q – the reaction energy yield, E_d – the kinetic energy of incident deuteron. For convenience we introduce the coefficient connecting the coordinate systems G:

$$G = \frac{|1+\beta\cos\theta|}{\left(1+\beta^2+2\beta\cos\theta\right)^{\frac{3}{2}}}.$$

The measured yield of α-particles Y of $^{10}B(d,\alpha_0)^8Be$, $^{10}B(d,\alpha_1)^8Be^*$, $^{10}B(d,p_2)^9Be^*$, $^{11}B(d,\alpha_0)^9Be$, and $^{11}B(d,\alpha_2)^9Be^*$ reactions at 135° and 168° are presented in Table 1.

The measurements were carried out in 100 keV deuteron beam energy steps. The measured energy of the deuteron beam differed from the set energy by no more than 2 keV; energy stability was 1–2 keV. When the deuteron passes through the boron layer, the deuteron loses energy from 15 keV at the energy of 2.2 MeV to 41 keV at the energy of 0.4 MeV (taking into account the presence of nitrogen in the boron layer). Table 1 gives exactly this deuteron energy, namely the average energy in the boron layer, not the energy of the incident deuteron at the boron surface.

5. $^{10}B(d,\alpha_0)^8Be$ reaction

The data obtained make it possible to determine the differential cross-section of the $^{10}B(d,\alpha_0)^8Be$ reaction; it is given in Fig. 2 and in Tables 2 and 3. The accuracy of cross-section measurement is determined by the accuracy of boron thickness determination (10 %), the accuracy of deuteron fluence determination (1 %), the accuracy of solid angle determination (5 %), and statistical uncertainty (9–34 %); in total it is 11–34 %.

The differential cross-section we obtained almost perfectly coincides with the data given in [2] at the angle 168° and expands the energy range. Our measured data at the angle of 168° agrees well with the data given in [4] and slightly exceeds the data given in [2]. It is noticeable that the reaction proceeds non-isotropically.

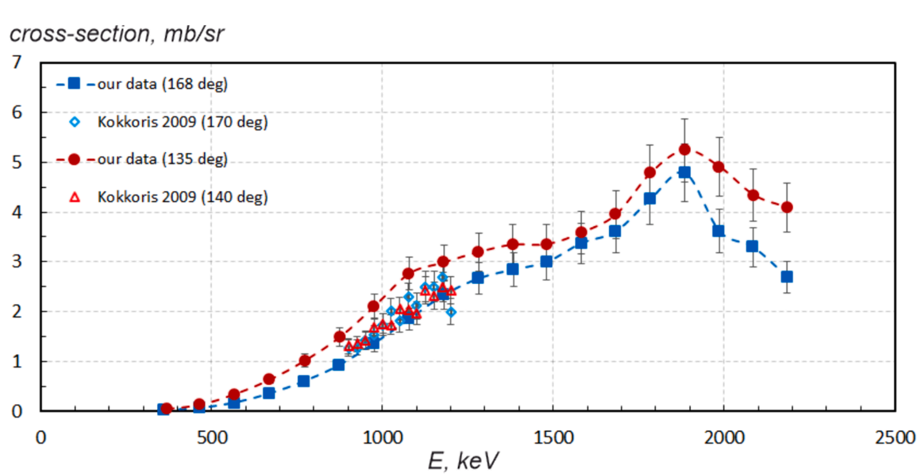

Fig. 3. The measured differential cross-section of the $^{11}B(d,\alpha_0)$. Differential cross-sections are in the center-of-mass system.

Table 4
The differential cross-section of the $^{11}B(d,\alpha_0)^9Be$ reaction (in the center-of-mass system) at 135°: E – the deuteron energy, ΔE – the standard deviation of E, σ – the cross-section, Δσ – the statistical variance of σ.

E, keV	ΔE, keV	σ, mb/sr	Δσ, mb/sr
369	41	0.05	0.02
467	35	0.13	0.02
567	33	0.34	0.04
671	30	0.63	0.08
773	28	1.0	0.1
875	26	1.5	0.2
977	24	2.1	0.3
1078	23	2.8	0.3
1180	22	3.0	0.4
1282	20	3.2	0.4
1382	20	3.3	0.4
1481	19	3.4	0.4
1583	18	3.6	0.4
1684	17	4.0	0.5
1784	17	4.8	0.6
1885	16	5.2	0.6
1987	15	4.9	0.6
2087	15	4.3	0.5
2185	15	4.1	0.5

Table 5
The differential cross-section of the $^{11}B(d,\alpha_0)^9Be$ (in the center-of-mass system reaction) at 168°: E – the deuteron energy, ΔE – the standard deviation of E, σ – the cross-section, Δσ – the statistical variance of σ.

E, keV	ΔE, keV	σ, mb/sr	Δσ, mb/sr
360	41	0.018	0.011
467	35	0.064	0.008
567	33	0.17	0.02
670	30	0.35	0.04
772	28	0.60	0.07
874	26	0.9	0.1
977	24	1.4	0.2
1078	23	1.9	0.2
1180	22	2.3	0.3
1282	20	2.7	0.3
1383	20	2.8	0.3
1481	19	3.0	0.4
1583	18	3.4	0.4
1683	17	3.6	0.4
1784	17	4.3	0.5
1885	16	4.8	0.6
1987	15	3.6	0.4
2085	15	3.3	0.4
2185	15	2.7	0.3

Table 6
The differential cross-section of the $^{11}B(d,\alpha_2)^9Be^*$ reaction (in the center-of-mass system) at 135°: E – the deuteron energy, ΔE – the standard deviation of E, σ – the cross-section, Δσ – the statistical variance of σ.

E, keV	ΔE, keV	σ, mb/sr	Δσ, mb/sr
369	41	0.05	0.02
467	35	0.14	0.06
567	33	0.30	0.08
671	30	0.5	0.2
773	28	0.7	0.2
875	26	1.0	0.2
977	24	1.7	0.2
1078	23	1.9	0.4
1180	22	2.0	0.3
1282	20	2.3	0.4
1382	20	2.8	0.4
1481	19	2.9	0.5
1583	18	2.6	0.3
1684	17	2.4	0.4
1784	17	2.7	0.4
1885	16	2.9	0.8
1987	15	2.7	0.4
2087	15	2.8	0.5
2185	15	2.7	0.5

Table 7
The differential cross-section of the $^{11}B(d,\alpha_2)^9Be^*$ reaction (in the center-of-mass system) at 168°: E – the deuteron energy, ΔE – the standard deviation of E, σ – the cross-section, Δσ – the statistical variance of σ.

E, keV	ΔE, keV	σ, mb/sr	Δσ, mb/sr
360	41	0.023	0.009
467	35	0.07	0.01
567	33	0.16	0.02
670	30	0.27	0.05
772	28	0.40	0.09
874	26	0.53	0.09
977	24	0.66	0.09
1078	23	1.0	0.2
1180	22	1.2	0.2
1282	20	1.3	0.2
1383	20	1.5	0.2
1481	19	1.5	0.2
1583	18	1.4	0.2
1683	17	1.4	0.2
1784	17	1.6	0.2
1885	16	1.6	0.2
1987	15	1.6	0.2
2085	15	2.0	0.3
2185	15	1.7	0.2

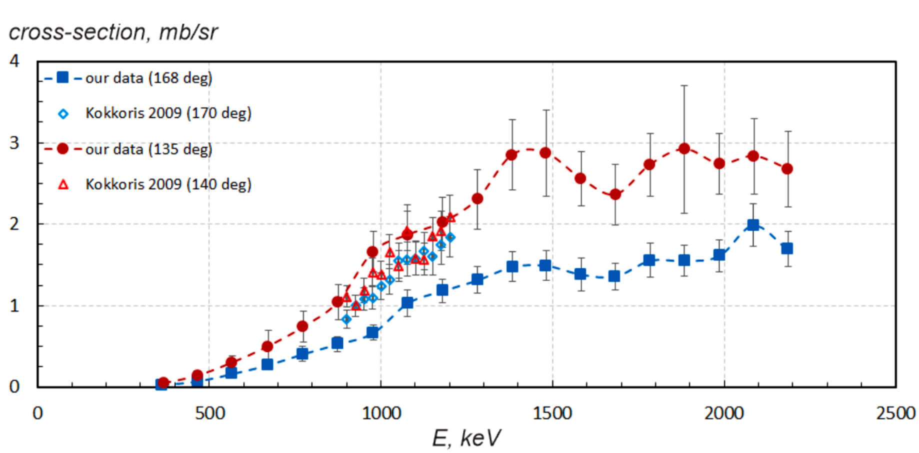

Fig. 4. The measured differential cross-section of the $^{11}B(d,\alpha_2)^9Be^*$. Differential cross-sections are in the center-of-mass system.

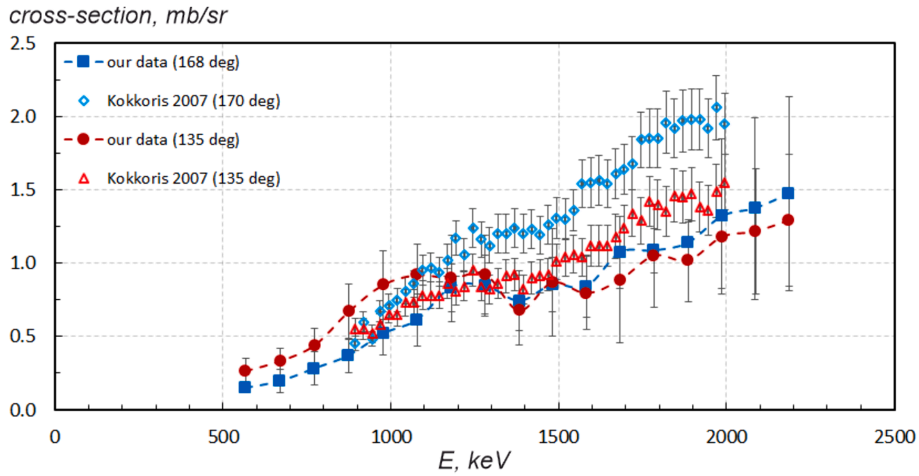

Fig. 5. The measured differential cross-section of the $^{10}B(d,p_2)^{11}B^*$ reaction (in the center-of-mass system).

Table 8
The differential cross-section of the $^{10}B(d,p_2)^{11}B^*$ reaction (in the center-of-mass system) at 135°: E – the deuteron energy, ΔE – the standard deviation of E, σ – the cross-section, Δσ – the statistical variance of σ.

E, keV	ΔE, keV	σ, mb/sr	Δσ, mb/sr
567	33	0.26	0.08
671	30	0.33	0.09
773	28	0.4	0.1
875	26	0.7	0.2
977	24	0.9	0.2
1078	23	0.9	0.2
1180	22	0.9	0.3
1282	20	0.9	0.3
1382	20	0.7	0.2
1481	19	0.9	0.4
1583	18	0.8	0.3
1684	17	0.9	0.4
1784	17	1.1	0.4
1885	16	1.0	0.3
1987	15	1.2	0.4
2087	15	1.2	0.4
2185	15	1.3	0.5

Table 9
The differential cross-section of the $^{10}B(d,p_2)^{11}B^*$ reaction (in the center-of-mass system) at 168°: E – the deuteron energy, ΔE – the standard deviation of E, σ – the cross-section, Δσ – the statistical variance of σ.

E, keV	ΔE, keV	σ, mb/sr	Δσ, mb/sr
567	33	0.15	0.02
670	30	0.19	0.08
772	28	0.9	0.1
874	26	0.4	0.1
977	24	0.5	0.2
1078	23	0.6	0.2
1180	22	0.8	0.2
1282	20	0.8	0.2
1383	20	0.7	0.2
1481	19	0.9	0.2
1583	18	0.8	0.2
1683	17	1.1	0.3
1784	17	1.1	0.2
1885	16	1.1	0.1
1987	15	1.3	0.5
2085	15	1.4	0.6
2185	15	1.5	0.7

6. $^{11}B(d,\alpha_0)^9Be$ reaction

The data obtained make it possible to determine the differential cross-section of the $^{11}B(p,\alpha_0)^9Be$ reaction; it is given in Fig. 3 and in Tables 4 and 5. The accuracy of cross-section measurement is determined by the accuracy of boron thickness determination (10 %), the accuracy of deuteron fluence determination (1 %), the accuracy of solid angle determination (5 %), the accuracy in counting the number of events at energies above 1.4 MeV (3 %), and statistical uncertainty (2–32 %); in total it is 12–32 %.

The differential cross-section we measured is consistent with the data given in the article [19] in the energy range of 900 – 1200 keV, and provide data for deuteron energies below 900 keV and above 1200 keV for the first time.

7. $^{11}B(d,\alpha_2)^9Be^*$

The data obtained make it possible to determine the differential cross-section of the $^{11}B(d,\alpha_2)^9Be^*$ reaction; it is given in Fig. 4 and in Tables 6 and 7. The accuracy of cross-section measurement is determined by the accuracy of boron thickness determination (10 %), the accuracy of deuteron fluence determination (1 %), the accuracy of solid angle determination (5 %), the accuracy in counting the number of events at energies above 1.4 MeV (3 %), and statistical uncertainty (8–40 %); in total it is 12–40 %.

The differential cross-section we measured is consistent with the data given in the article [19] at the angle 135° in the energy range of 900–1200 keV. Our measured data at the angle of 168° is below the data given in [19]. Our measured data provide data for deuteron energies below 900 keV and above 1200 keV for the first time.

8. $^{10}B(d,p_2)^{11}B^*$

The data obtained make it possible to determine the differential cross-section of the $^{10}B(d,p_2)^{11}B^*$ reaction; it is given in Fig. 5 and in Tables 8 and 9. The accuracy of cross-section measurement is determined by the accuracy of boron thickness determination (10 %), the accuracy of deuteron fluence determination (1 %), the accuracy of solid angle determination (5 %), the accuracy in counting the number of events at energies above 1.4 MeV (3 %), and statistical uncertainty (13–48 %); in total it is 13–48 %.

The differential cross-section we measured is consistent with the data given in the article [2] with the exception of the angle of 168° degrees at energies above 1400 keV – in this region our data is slightly lower. Due to the complex composition of the spectrum, there are large uncertainties in the results.

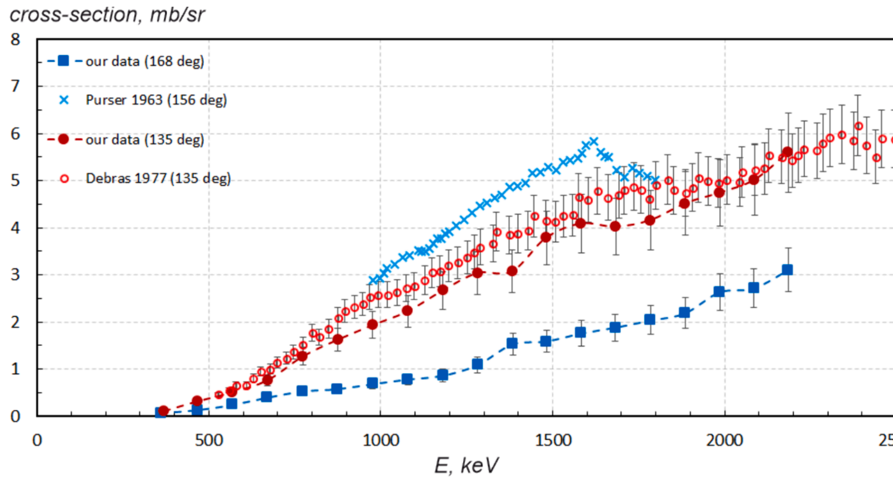

Fig. 6. The measured differential cross-section of the $^{10}B(d,\alpha_1)^8Be^*$ reaction (in the center-of-mass system).

Table 10
The differential cross-section of the $^{10}B(d,\alpha_1)^8Be^*$ reaction (in the center-of-mass system) at 135°: E – the deuteron energy, ΔE – the standard deviation of E, σ – the cross-section, Δσ – the statistical variance of σ.

E, keV	ΔE, keV	σ, mb/sr	Δσ, mb/sr
369	41	0.11	0.02
467	35	0.32	0.05
567	33	0.51	0.08
671	30	0.8	0.1
773	28	1.3	0.2
875	26	1.6	0.2
977	24	1.9	0.3
1078	23	2.2	0.3
1180	22	2.7	0.4
1282	20	3.0	0.5
1382	20	3.1	0.5
1481	19	3.8	0.6
1583	18	4.1	0.6
1684	17	4.0	0.6
1784	17	4.2	0.6
1885	16	4.5	0.7
1987	15	4.7	0.7
2087	15	5.0	0.8
2185	15	5.6	0.8

Table 11
The differential cross-section of the $^{10}B(d,\alpha_1)^8Be^*$ reaction (in the center-of-mass system) at 168°: E – the deuteron energy, ΔE – the standard deviation of E, σ – the cross-section, Δσ – the statistical variance of σ.

E, keV	ΔE, keV	σ, mb/sr	Δσ, mb/sr
360	41	0.07	0.01
467	35	0.14	0.02
567	33	0.25	0.04
670	30	0.40	0.06
772	28	0.53	0.08
874	26	0.58	0.09
977	24	0.7	0.1
1078	23	0.8	0.1
1180	22	0.9	0.1
1282	20	1.1	0.2
1383	20	1.5	0.2
1481	19	1.6	0.2
1583	18	1.8	0.3
1683	17	1.9	0.3
1784	17	2.0	0.3
1885	16	2.2	0.3
1987	15	2.6	0.4
2085	15	2.7	0.4
2185	15	3.1	0.5

9. $^{10}B(d,\alpha_1)^8Be^*$

The data obtained make it possible to determine the differential cross-section of the $^{10}B(d,\alpha_1)^8Be^*$ reaction; it is given in Fig. 6 and in Tables 10 and 11. The accuracy of cross-section measurement is determined by the accuracy of boron thickness determination (10 %), the accuracy of deuteron fluence determination (1 %), the accuracy of solid angle determination (5 %), the accuracy in counting the number of events at energies above 1.4 MeV (3 %), and statistical uncertainty (5–15 %); in total it is 15 %.

The differential cross-section we measured is consistent with the data given in articles [4] at the angle 135° and several times lower than the data given in articles [8] at the angle 168°. We assume, based on the obtained data, that this cross–section is characterized by non-isotropy.

10. Conclusion

The deuteron-boron fusion reaction produces many different charged particles. Data on the reactions cross-sections differ among different authors. We measured the energy spectrum of the reaction products of the deuteron boron interaction at deuteron energies up to 2.2 MeV for two angles of 135° and 168°. The obtained data allowed us to determine the differential cross-sections of the $^{10}B(d,\alpha_0)^8Be$, $^{10}B(d,\alpha_1)^8Be^*$, $^{10}B(d,p_2)^9Be^*$, $^{11}B(d,\alpha_0)^9Be$, $^{11}B(d,\alpha_2)^9Be^*$ reactions.

Funding

This work was supported by the Russian Science Foundation (grant number 19-72-30005).

CRediT authorship contribution statement

Sergey Taskaev: Writing – review & editing, Supervision, Conceptualization. **Victor Bessmeltsev:** Methodology, Investigation. **Marina Bikchurina:** Writing – original draft, Validation, Investigation, Formal analysis, Data curation. **Timofey Bykov:** Software. **Dmitrii Kasatov:** Methodology, Investigation. **Iaroslav Kolesnikov:** Investigation. **Alexey Nikolaev:** Methodology, Investigation. **Efim Oks:** Methodology, Investigation. **Georgii Ostreinov:** Writing – original draft, Validation, Formal analysis. **Sergey Savinov:** Writing – review & editing, Supervision, Conceptualization. **Anna Shuklina:** Investigation, Formal analysis, Data curation. **Evgeniia Sokolova:** Writing – original draft, Methodology, Investigation. **Georgy Yushkov:** Investigation.

Declaration of competing interest

The authors declare that they have no known competing financial interests or personal relationships that could have appeared to influence the work reported in this paper.

Data availability

Data will be made available on request.

References

[1] Jingsheng Yan, F.E. Cecil, J.A. McNeil, M.A. Hofstee, P.D. Kunz, Deuteron-induced reactions on ^{9}Be, ^{10}B, and ^{11}B at low energies, Phys. Rev. C 55 (1997) 1890–1918, https://doi.org/10.1103/PhysRevC.55.1890.

[2] M. Kokkoris, V. Foteinou, G. Provatas, et al., A detailed study of the d + ^{10}B system for nuclear reaction analysis – part A: the ^{10}B(d,p)^{11}B reaction in the energy region $E_{d,lab}$ = 900–2000 keV, Nucl. Instrum. Methods Phys. Res. B 263 (2) (2007) 357–368, https://doi.org/10.1016/j.nimb.2007.07.003.

[3] W. Buck, T. Rohwer, G. Staudt, A. Ziemke, F. Vogler, Observation of the isoscalar giant resonance in the reaction ^{10}B(d,α)^{8}Be(g.s.), Nucl. Phys. A 297 (2) (1978) 231–236, https://doi.org/10.1016/0375-9474(78)90273-7.

[4] G. Debras, G. Deconninck, Light elements analysis and application to glass industry, J. Radioanal. Chem. 38 (1977) 193–204, https://doi.org/10.1007/BF02520197.

[5] V. Valkovic, D. Miljanic, R.B. Liebert, G.C. Phillips, Energy dependence of the cross sections for the d+^{10}B → 3α and the p^{+1}1B → 3α reactions, Nucl. Phys. A 239 (2) (1975) 260–270, https://doi.org/10.1016/0375-9474(75)90450-9.

[6] R. Roy, J. Birchall, B. Frois, U. Von Moellendorff, C.R. Lamontagne, R. J. Slobodrian, Final state interaction and direct features of the 9Be(τ,α)αα and 10B (d,α)αα reactions, Nucl. Phys. A 245 (1) (1975) 87–106, https://doi.org/10.1016/0375-9474(75)90083-4.

[7] M. Lattuada, R. Potenza, Absolute differential cross-section of the^{10}B(d,α)^{8}Be reactions at E_d = 1.83 MeV, Lett. Nuovo Cimento 11 (1974) 662–664, https://doi.org/10.1007/BF02763141.

[8] K.H. Purser, B.H. Wildenthal, The B^{10}(d,α)Be^{8} reaction and the 2.94 MeV state in Be^{8}, Nucl. Phys. 44 (1963) 22–23, https://doi.org/10.1016/0029-5582(63)90003-8.

[9] J.R. Erskine, C.P. Browne, Isotopic-spin selection rule violation in the B10(d,α)Be8 reaction, Phys. Rev. 123 (1961) 958–967, https://doi.org/10.1103/PhysRev.123.958/.

[10] G.J.F. Legge, A search for fine structure in the reactions B^{10}(d, $_{α}$0)B^{e}8 and ^{B1}0(d, α1)^{Be}8*, Nucl. Phys. 26 (4) (1961) 608–615, https://doi.org/10.1016/0029-5582(61)90209-7.

[11] R.L. Becker, Angular distributions of B^{10}(d,α)Be^{8} reactions from 0.6 to 1.5 Mev, Phys. Rev. 119 (1960) 1076, https://doi.org/10.1103/PhysRev.119.1076.

[12] J.B. Marion, G. Weber, Compound nucleus effects in deuteron reactions: B10(d,p) B11 and B10(d,α)Be8, Phys. Rev. 103 (5) (1956) 1408, https://doi.org/10.1103/PhysRev.103.1408.

[13] F.E. Cecil, R.F. Fahlsing, Back-angle differential cross section measurements for (d,) reactions on light nuclei at low bombarding energies, Phys. Rev. C 24 (4) (1981) 1769, https://doi.org/10.1103/PhysRevC.24.1769.

[14] M.N.H. Comsan, A.A. El Kamhawy, M.A. Farouk, et al., The mechanism of the reaction B^{10}(d, p)^{B1}1 at low deuteron energies, Atomkernenergie 32 (1978) 189.

[15] N. Arena, G. Calvi, S. Cavallaro, et al., Absolute differential cross-section of the ^{9}Be (d,p)^{10}Be and ^{10}B(d,p)^{11}B reactions at deuteron energy $E_d \leq 2.5$ MeV, Lett. Nuovo Cimento 5 (1972) 879–882, https://doi.org/10.1007/BF02832812.

[16] D.L. Powell, G.M. Crawley, B.V.N. Rao, B.A. Robson, Deuteron-induced reactions in ^{6}Li, ^{9}Be and ^{10}B at bombarding energies of 4.5 to 6.0 MeV, Nucl. Phys. A 147 (1) (1970) 65–80, https://doi.org/10.1016/0375-9474(70)90510-5.

[17] R.V. Poore, P.E. Shearin, D.R. Tilley, et al., Differential cross sections of ^{12}C(d, p$_1$)^{13}C and ^{10}B(d,p)^{11}B below E_d = 3.0 MeV, Nucl. Phys. A 92 (1) (1967) 97–122, https://doi.org/10.1016/0375-9474(67)90678-1.

[18] G.R. Harrison, G.D. Schmidt, C.D. Curtis, Differential and total cross sections of the B10(*d*, *p*)B11 reaction at low-deuteron energies, Phys. Rev. 117 (2) (1960) 532, https://doi.org/10.1103/PhysRev.117.532.

[19] M. Kokkoris, M. Diakaki, P. Misaelides, et al., Study of the d + ^{11}B system differential cross-sections for NRA purposes, Nucl. Instrum. Methods Phys. Res. Sect. B 267 (8–9) (2009) 1740–1743, https://doi.org/10.1016/j.nimb.2009.01.087.

[20] D. Sargood, G. Putt, Angular distributions in the reactions ^{11}B(d, p$^{)1}$2B and ^{1}1B(d, ^{a})9Be, Australian J. Phys. 18 (5) (1965) 491–496, https://doi.org/10.1071/PH650491.

[21] R.A. August, H.R. Weller, D.R. Tilley, Radiative deuteron capture into the secondary doorway state of ^{13}C, Phys. Rev. C 32 (4) (1985) 1420, https://doi.org/10.1103/PhysRevC.32.1420.

[22] H.R. Weller, R.A. Blue, The ^{13}C(d, $_{γ}$0$)^{1}$5N and the ^{1}1(d, γ$^{0)}$13C cross sections in the region of the giant dipole resonance, Nucl. Phys. A 211 (2) (1973) 221–231, https://doi.org/10.1016/0375-9474(73)90715-X.

[23] R.M. Tisinger Jr., P.W. Keaton, G.E. Owen, Differential cross sections for the reaction B^{11}(*d*,*p*)B^{12} for E_D=1−2.6 MeV, Phys. Rev. 135 (1964) B892, https://doi.org/10.1103/PhysRev.135.B892.

[24] H.T. Aslani, A.A. Mehmandoost-Khajeh-Dad, A. Jokar, H. Rafi-kheiri, Differential cross-section measurements of the ^{11}B(d,pγ$_{1,2}$)^{12}B reactions for analytical applications, Nucl. Instrum. Methods Phys. Res. Sect. B 540 (2023) 141–147, https://doi.org/10.1016/j.nimb.2023.04.033.

[25] G.Á. Sziki, A. Simon, Z. Szikszai, Z.S. Kertész, E. Dobos, Gamma ray production cross-sections of deuteron induced nuclear reactions for light element analysis, Nucl. Instrum. Methods Phys. Res. Sect. B 251 (2) (2006) 343–351, https://doi.org/10.1016/j.nimb.2006.07.008.

[26] S. Taskaev, V. Bessmeltsev, M. Bikchurina, T. Bykov, D. Kasatov, Ia Kolesnikov, A. Nikolaev, E. Oks, G. Ostreinov, S. Savinov, A. Shuklina, E. Sokolova, G. Yushkov, Measurement of the ^{11}B(p,α$_0$)^{8}Be and the ^{11}B(p,α$_1$)^{8}Be* reactions cross-sections at the proton energies up to 2.2 MeV, Nucl. Instrum. Methods Phys. Res. Sect. B 555 (2024) 165490, https://doi.org/10.1016/j.nimb.2024.165490.

[27] S. Taskaev, E. Berendeev, M. Bikchurina, T. Bykov, D. Kasatov, I. Kolesnikov, A. Koshkarev, A. Makarov, G. Ostreinov, V. Porosev, S. Savinov, I. Shchudlo, E. Sokolova, I. Sorokin, T. Sycheva, G. Verkhovod, Neutron source based on vacuum insulated tandem accelerator and lithium target, Biology 10 (2021) 350, https://doi.org/10.3390/biology10050350.

[28] S. Taskaev, Accelerator-based Neutron Source VITA, FizMatLit, Moscow, 2024.

[29] S. Taskaev, M. Bikchurina, T. Bykov, D. Kasatov, Ia Kolesnikov, G. Ostreinov, S. Savinov, E. Sokolova, Measurement of cross-section of the ^{6}Li(d,α)^{4}He, ^{6}Li(d, p)^{7}Li, ^{6}Li(d,p)^{7}Li*, ^{7}Li(d,α)^{5}He, and ^{7}Li(d,nα)^{4}He reactions at the deuteron energies from 0.3 MeV to 2.2 MeV, Nucl. Instrum. Methods Phys. Res. Sect. B 554 (2024) 165460, https://doi.org/10.1016/j.nimb.2024.165460.

[30] Tables of Physical Constants. Handbook. I.K. Kikoin Edition, AtomIzdat, Moscow (1976).

[31] Y. Shirokov, N. Yudin, Nuclear Physics. Volumes 1 and 2, MIR Publishers, Moscow, 1982.